DOI: 10.1021/ma901322t

Macromolecules
ARTICLE

Impact of Cross-Linking Density and Glassy Chain Dynamics on Pore Stability in Mesoporous Poly(styrene)

Jens Weber*,† and Lennart Bergström

Department of Physical, Inorganic and Structural Chemistry, Arrhenius Laboratory, Stockholm University, S-106 91 Stockholm, Sweden. †Present address: Department of Colloid Chemistry, Max Planck Institute of Colloids and Interfaces, D-14424, Potsdam, Germany.

Received June 19, 2009; Revised Manuscript Received September 30, 2009

ABSTRACT: Mesoporous poly(styrene) (PS) containing various amounts of the cross-linker divinylbenzene was synthesized by a hard-templating routine using pressed pellets of fumed silica as templates. Porous polymers with a surface area of 215 $m^2 g^{-1}$ and porosities up to ~35 vol % could be obtained. The impact of the cross-linker content and the processing on the porosity of the materials was investigated by nitrogen sorption and small-angle X-ray scattering. The surface area of the nascent porous PS increases and the pore size decreases with increasing amount of cross-linker. Furthermore, it was found that the porous polymers lose surface area at temperatures that are substantially below the glass transition temperature, T_g, of bulk polystyrene. The loss in surface area at temperatures below 65 °C suggests that partial pore collapse also may be induced in the glassy state. Finally, the stability of the mesopores against solvent swelling was investigated. A critical pore collapse was found at a cross-linker content of ~20 wt %. In this context, also the existence of traced porosity, i.e., a nonaccessible mesostructure or porosity, could be confirmed.

Introduction

During the past decades, much effort has been spent on the exploration of meso- and microporous materials given their high importance in various technologies, including separation technology and catalysis. Most of the work has been done using inorganic materials, i.e., mesoporous silica and metal oxides as well as carbonaceous materials.[1−4] It was only during the past years that substantial work has also been done in the area of polymers,[5−7] but there still is plenty of uncharted terrain in the area of mesoporous polymers.

In general, mesoporous polymers, i.e., polymers possessing pore sizes between 2 and 50 nm, can be synthesized via templating approaches. The self-assembly of block copolymers followed by cross-linking of one block and removal of the other one can lead to mesoporous polymers.[5,8] This approach can be regarded as one case of "soft templating". Other forms of soft templating (e.g., the use of surfactants), which proved to be very successful for the synthesis of mesostructured inorganic materials, could be used only for a limited amount of polymeric systems because of thermodynamic reasons.[9] Usually, demixing processes take place which result in a loss of morphological control. However, it is not impossible to use well-controlled phase separation processes to obtain mesoporous polymers.[10]

The use of hard templates, e.g., mesostructured silica, for the synthesis of mesoporous polymers has therefore several advantages, as it does not require the use of (sometimes) expensive block copolymers. Consequently, several examples of the use of hard templates for the synthesis of mesoporous polymers are known.[6,11−14] In addition to those examples which employ mostly regular-shaped templates as spherical silica nanoparticles or block copolymer templated mesoporous silica, also irregular-shaped fumed silica has been used as a hard template in the synthesis of melamine resins.[15,16]

*Corresponding author: Tel +49-331-5679569; Fax +49-331-5679502; e-mail jensw@inorg.su.se, jens.weber@mpikg.mpg.de.

Mesoporous poly(styrene) (PS) and PS networks may be synthesized by both block copolymer templating and hard templating.[13,17] However, up to now, there is no comprehensive study on the impact of cross-linking degree or the processing protocol on the porosity but just the description of their synthesis. Despite those polymers with well-defined pore sizes prepared by templating, it is also possible to synthesize mesoporous PS networks by a careful control of the phase separation process.[10,18] The drawback of such methodology is, however, that it is not universal; i.e., the exact parameters have to be carefully adjusted again if different monomers are used.

Even though a considerable amount of work devoted to the synthesis of mesoporous polymers has been performed, there have been only a few works regarding the stability of mesopores in polymers.[19−21] It was shown that most often a well-defined stability criterion exists, i.e., a critical cross-linking density. If this threshold value is not exceeded, pore collapse takes place. However, there are a still a lot of open questions that need to be answered. Among them is the influence of the processing and the template removal on the observable porosity, and it is therefore one of the aims of the present study to extent the knowledge about pore stability.

Here, we present a systematic study of mesoporous poly(styrene) (PS) and mesoporous PS networks that covers the synthesis by a hard-templating approach and an extensive characterization of the resulting polymers. The template was produced from commercially available fumed silica powder that has been pressed into pellets. The cross-linker density was varied and the mesoporous PS was analyzed by means of nitrogen sorption, small-angle X-ray scattering (SAXS), electron microscopy, infrared spectroscopy, and thermal analysis. Furthermore, the stability of the polymers against solvent swelling was investigated.

Materials and Methods

Materials. Fumed silica (primary particle size: 14 nm; Aldrich: S5505), styrene (99%), divinylbenzene (DVB, technical

 Published on Web 10/12/2009

grade, 80%) and 2,2′-azobis(2-methylpropionitrile) (AIBN, 98%) were purchased from Aldrich. Styrene and DVB were purified by washing with 1 M aqueous NaOH and water followed by drying over Na_2SO_4 and passing through activated, basic alumina. AIBN was used as received.

Typical Synthesis of Mesoporous Poly(styrene) and Poly(styrene-*co*-divinylbenzene) Networks. Approximately 150 mg of fumed silica was pressed to a pellet using a hydraulic pellet press at an average pressure of 9 MPa. 1.5 g of the monomer mixture containing 2 wt % AIBN was deaired by bubbling with nitrogen for a few minutes. The silica pellets were infiltrated with this mixture and transferred without removing excess monomer from the outside into a 10 mL flask which was purged with nitrogen. After sealing the flask with a septum, polymerization was initiated by heating the flasks to 65 °C for 18−20 h. After cooling to room temperature, the hybrid material was broken into smaller pieces, and the silica was removed by treatment with a 1 M sodium hydroxide solution for 3 days. Afterward, the mesoporous PS was purified by extensive washing with deionized water and finally dried under vacuum at room temperature. The successful removal of the template was verified by thermogravimetric analysis and infrared spectroscopy. It is worth noting that the dried materials usually did not sink down in water upon immersion but floated on top; i.e., they did not show an immediate uptake of water.

Methods. Nitrogen sorption isotherms were measured at 77 K using a Micromeritics ASAP 2020 machine after degassing the samples under vacuum for at least 20 h.

SAXS curves were recorded at room temperature with a Nonius rotating anode instrument (4 kW, Cu Kα) with pinhole collimation and a MARCCD detector (pixel size: 79). The distance between sample and detector was 74 cm, covering a range of the scattering vector $s = 2/\lambda \sin(\theta) = 0.04-0.7$ nm^{-1} (2θ = scattering angle, $\lambda = 0.154$ nm). 2D diffraction patterns were transformed into a 1D radial average of the scattering intensity. The SAXS patterns obtained from polymer and hybrid samples were corrected for scattering contributions arising from 3D electron density fluctuations as suggested by Perret and Ruland before being further analyzed.[22]

FT-infrared spectra were acquired using a Varian 670-IR spectrometer equipped with a GoldenGate ATR device. Thermogravimetric analysis (TGA) was performed under air using a Perkin-Elmer TGA7. DSC analysis was performed using a Mettler-Toledo DSC1. Gel permeation chromatography (GPC) was done in THF using simultaneous UV and RI detection. Calibration was done with poly(styrene) standards.

Scanning electron microscopy was done on a Jeol JSM-7000F FE-SEM machine at an acceleration voltage of 15 kV. Samples were coated with carbon prior to analysis. Transmission electron microscopy (TEM) was performed using a Jeol JEM-3010 at an accelerating voltage of 300 kV. Suitable samples of the mesoporous polymers were prepared by mild grinding and subsequent dispersion in acetone. A drop of the suspension was put on a copper grid and allowed to dry. Atomic force microscopy (AFM) was done on a Veeco MultiMode V. Images were recorded using tapping mode.

Theoretical Background

The analysis of the porous materials described in this paper is mainly based on two methods: nitrogen sorption and small-angle X-ray scattering (SAXS). We wish to give a short overview how we employ these techniques to extract information about the porosity.

Low-pressure nitrogen sorption at 77 K (boiling point of nitrogen) is one of the most common techniques for the analysis of porous materials. It allows the determination of the specific surface area, the average pore size and the pore size distribution (PSD), and the porosity ϕ.[23,24] The specific surface area is determined by consideration of multilayer adsorption of nitrogen on the surface using the well-established Brunauer−Emmer−Teller (BET) method. The determination of the mesopore size is based on the depression of the pressure at which condensation takes place in mesopores. The relation between the condensation pressure and the pore radius r is given by the Kelvin equation:

$$\ln\left(\frac{p}{p_0}\right) = -\frac{2\sigma V_L}{RT}\frac{1}{r_{pore}}\cos\Theta \tag{1}$$

with p/p_0 being the relative pressure, σ the interfacial tension of nitrogen, V_L the molar volume of nitrogen, and Θ the contact angle of the condensed nitrogen.

Average pore sizes and PSDs are calculated using the Barrett−Joyner−Halenda (BJH) approach which is based on the Kelvin equation. It should be noted that this approach is based on the assumption of cylindrical mesopores. Commonly, a hysteresis is observed upon desorption of nitrogen. The shape of this hysteresis is related to morphological details of the pores, and several classifications exist.[23]

The porosity ϕ is the volume fraction of the pores in the material and can be determined from the total volume of nitrogen adsorbed and condensed in the pores:

$$\phi = \frac{V_{pore}}{V_{pore} + V_{pore\ wall}} \tag{2}$$

Next to gas sorption, scattering methods are a major tool for the characterization of porous materials. SAXS is a versatile method for the investigation of porous materials as it can also give information about the interfacial area, pore and pore wall sizes, etc.[14,25] Generally, any two-phase system exhibits a decay of the scattering intensity $I(s)$ with the power of −4, where $s = 2\lambda^{-1}\sin(\theta)$ is the scattering vector, λ the wavelength of the X-rays, and θ the scattering angle. This decay is known as the Porod law or behavior and allows the extraction of the Porod length l_p:[22]

$$l_p = \frac{4\pi\int_0^\infty s^2 I(s)\,ds}{2\pi^3 \lim_{s\to\infty} s^4 I(s)} \tag{3}$$

The Porod law is connected to the interface area S of the enlightened volume V and to the number-averaged pore size $\langle l_{pore}\rangle$ and pore wall $\langle l_{wall}\rangle$ size through the porosity ϕ:

$$\frac{S}{V} = \frac{4\phi(1-\phi)}{l_p} \tag{4}$$

$$\frac{1}{l_p} = \frac{1}{(1-\phi)\langle l_{pore}\rangle} = \frac{1}{\phi\langle l_{wall}\rangle} \tag{5}$$

The main advantage of pore sizes $\langle l_{pore}\rangle$ determined by SAXS is their model independency; i.e., they are not dependent on any underlying geometrical assumption. Despite those features that apply for every two-phase system, there are additional features which can be related to the geometrical shape of the scattering objects (e.g., platelets, cylinders, spheres, etc.), but those will not be covered here.

Results and Discussion

Characterization of the Template and the Inorganic/Organic Hybrid Materials. Fumed silica is typically produced by flame pyrolysis of $SiCl_4$ at very high temperatures, and as a consequence the particles possess an irregular shape (Figure S3). The specific surface area of the as-received fumed silica powder was determined to ∼200 m^2 g^{-1}, which corresponds reasonably well with the nominal diameter of

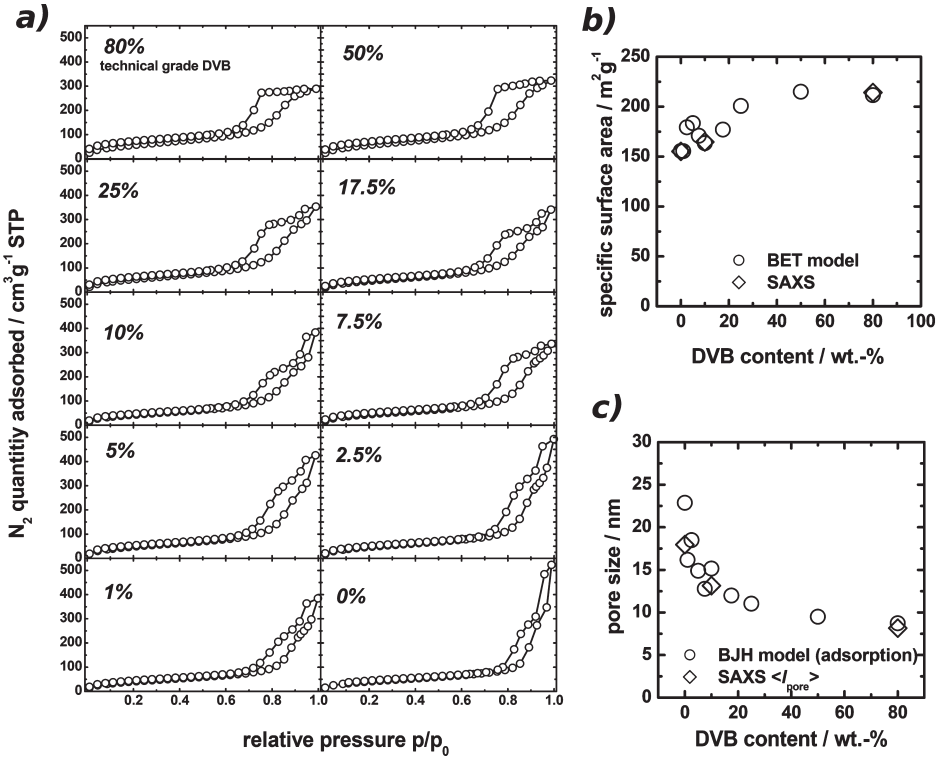

Figure 1. (a) Nitrogen sorption isotherms of samples containing various amount of divinylbenzene (DVB). (b) Specific surface areas (determined by the BET model or SAXS data evaluation) as a function of DVB content. (c) Pore sizes (determined by the BJH model using the adsorption branch or SAXS data evaluation) as a function of DVB content.

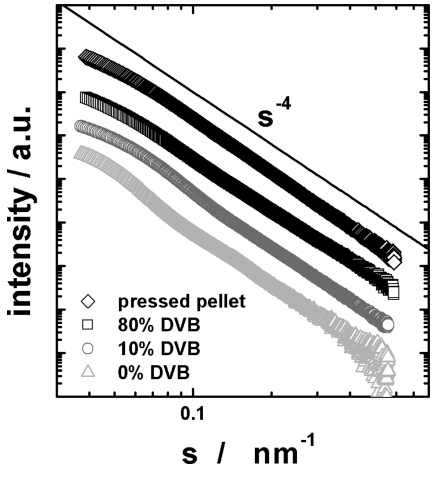

Figure 2. SAXS patterns of selected samples. The patterns of the polymers were corrected for 3D electron density fluctuations. The solid line has a slope of −4 (Porod's law).

14 nm given by the manufacturer. The isotherm did not show any distinct hysteresis and was of type II, according to the IUPAC definition.[23] No mesoporosity could be observed, and there was no evidence of any microporosity. The fumed silica powder was consolidated to a pellet with a porosity ϕ = 0.69 by subjecting a powder assembly to an axial pressure of ~9 MPa. While the specific surface area remained virtually unaffected by the consolidation, the shape of the isotherm changed and a type IV hysteresis at high relative pressures was observed. This suggests that large mesopores originate from the interstices between the nanoparticles in the consolidated powder bodies.

The pressed pellet was also investigated by SAXS. No distinct features apart from a pronounced Porod behavior, which allowed the calculation of the Porod length l_p, was found (see Figure 2). Indeed, the pore characteristics and surface area obtained from the SAXS analysis of the pressed pellet ($\langle l_{pore} \rangle = 23.9$ nm, $\langle l_{wall} \rangle = 10.7$ nm, $S_{SAXS} = 178\ m^2\ g^{-1}$) are in good agreement with the data obtained by nitrogen sorption analysis. Details of the calculations as well as the complete analytical data can be found in the Supporting Information.

The infiltration of the monomer mixture into the pellets proceeded smooth and fast. The almost transparent, infiltrated pellets were then transferred into a 10 mL flask, and polymerization was induced by heating to 65 °C. Technical divinylbenzene (DVB; composition: ~80% DVB and ~20% of ethylstyrene isomers) was used as the cross-linker. The samples were named according to their DVB weight content. Fully cross-linked samples, i.e., samples without additional styrene, are termed PS80DVB. Samples with cross-linker contents of 80%, 50%, 25%, 17.5%, 10%, 7.5%, 5%, 2.5%, 1%, and 0% were synthesized and named as indicated before. It shall be noted that we use the nominal degree of cross-linking throughout the article for (i) clarity and (ii) due to the fact that the determination of the true degree of cross-linking is not trivial for the system under investigation.

After the polymerization step, the mainly monolithic, off-white hybrid materials were broken into pieces. The polymer content was determined by thermogravimetric analysis (TGA) and was found to vary between 52 and 45 wt %. On the basis of the porosity of the pressed pellet, the maximum polymer weight content was calculated to ~53 wt %. The highest polymer content was found for the sample PS80DVB, and the lowest polymer content was found for materials with low DVB content. The reason for this difference might be due to the higher volatility of styrene in comparison with DVB. This hypothesis is supported by nitrogen sorption measurements of hybrid materials

Table 1. Composition and Characteristics of the Pressed Fumed Silica Pellet and the "Nascent" Porous PS with Varying DVB Content

sample	polymer/silica [wt %]	V_{pore}[a] [cm^3 g^{-1}]	ϕ	S_{BET} [m^2 g^{-1}]	S_{SAXS} [m^2 g^{-1}]	d_{pore}[b] [nm]	$\langle l_{pore}\rangle$ [nm]	$\langle l_{wall}\rangle$ [nm]
pressed pellet	0/100	1.06	0.69	200.5	178	25	23.9	10.7
PS80 DVB	51.7/48.3	0.45	0.32	211.5	219	8.73	8.2	17.4
PS50DVB	51.0/49.0	0.5	0.34	215		9.5		
PS25DVB	47.9/52.1	0.55	0.36	200.7		11.03		
PS17.5DVB	46.9/53.1	0.53	0.36	177.0		11.99		
PS10DVB	44.4/55.6	0.59	0.38	163.4	180	15.15	13.1	21.1
PS7.5DVB	47.6/52.4	0.52	0.35	170.9		12.77		
PS5DVB	46.0/54.0	0.64	0.40	183.5		14.89		
PS2.5DVB	45.2/54.8	0.74	0.44	179.3		18.49		
PS1DVB	44.6/55.4	0.58	0.38	155.4		16.17		
PS0DVB	44.9/55.1	0.81	0.46	155.6	176	22.88	18.0	21.7

[a] Determined at $p/p_0 = 0.99$. [b] BJH average (analysis of the adsorption branch).

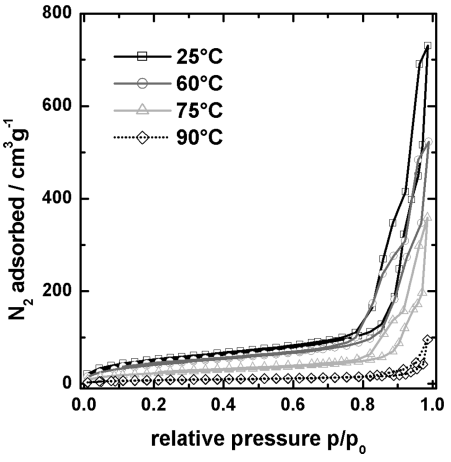

Figure 3. Nitrogen sorption isotherms of non-cross-linked PS after degassing for 20 h at 25, 60, 75, or 90 °C.

containing 10 and 5 wt % DVB, which revealed a low porosity ($S_{BET} \sim 19$ m^2 g^{-1}, pore volume ~ 0.1 cm^3 g^{-1}). The isotherms of those hybrid materials (Figure S5) resembled the shape of those measured for the pure pressed pellets, which is another support for partial pore emptying due to thermal evaporation. However, as the amount of emptied pores is low, we will not elaborate further on this.

Characterization of "Nascent" Mesoporous Polymers. Figure 1a represents the nitrogen sorption isotherms of the "nascent" mesoporous polymers, after removal of the silica template. It should be noted that the degassing was performed under high vacuum at only 60 °C, which is significantly lower than the glass transition temperature (T_g) of PS ($T_g \sim 100$ °C). All samples show a well-defined hysteresis at high relative pressures, which is a characteristic feature of mesopores. The samples PS80DVB and PS50DVB feature nonparallel adsorption and desorption branches. This behavior can be attributed to a complex pore structure where percolation phenomena of nitrogen filled pores play a role upon desorption.[23,26,27] Hence, we used the adsorption branch of the isotherm for determination of the PSD for all materials.[27] It should be noted that the isotherm shape of those samples is comparable to other examples of highly cross-linked, fumed silica templated polymer networks.[28]

However, when the amount of cross-linker (DVB) is 25 wt % or less, the adsorption and desorption branch become parallel, which suggests that the pore structure changes and that the pore connectivity increases. Furthermore, it was observed that the isotherms for those materials feature two inflection points, which indicate a bimodal pore size distribution. While the first major increase in adsorbed volume at low relative pressure can be attributed to the mesopores originating from the removal of the template, the second increase at $p/p_0 > 0.95$ might be related to pores that originate from incomplete filling or partial pore emptying of some interstices in the pressed silica pellet by the monomer solution as indicated in the section above.

Figure 1b shows that the specific surface areas for the porous PS range from 155 to 215 m^2 g^{-1}. The surface areas are the highest for the highly cross-linked samples and lower for samples of low cross-linking density.

Before discussing the pore size distribution (PSD) of the samples, we would like to emphasize the phenomenon of low-pressure hysteresis shortly. It was observed that the desorption branch of the isotherm does not reach the adsorption branch in the case of highly cross-linked samples; i.e., the isotherm is open, and not all adsorbed nitrogen can be removed upon desorption in the monitored pressure regime. Usually this feature is discussed in terms of structural rearrangements due to the softness of the materials. However, the highly cross-linked PS polymers have a high structural stability. We speculate that the high Laplace pressure associated with the capillary condensation within the mesopores at high relative pressures might lead to the dissolution of N_2 within the polymeric walls similar to the well-known dual mode sorption model.[29] The dissolved N_2 cannot be liberated easily as the pressure is decreased, and hence an open isotherm is observed. In the case of a lower cross-linking density, we suspect that the higher flexibility of those polymers reduces this effect.

In order to verify this hypothesis, we performed the following experiment. The nitrogen adsorption−desorption isotherm of PS80DVB was measured just up to a relative pressure of 0.3; i.e., no condensation of nitrogen in the mesopores occurred. We observed a hysteresis also in this measurement. However, the hysteresis was much smaller (volume difference between adsorption branch and desorption branch at $p/p_0 = 0.05$: ~ 5 cm^3 g^{-1} STP) than that observed for the full isotherm (volume difference at $p/p_0 = 0.05$: ~ 24 cm^3 g^{-1} STP). This can be regarded as an indirect proof of the above arguments. However, the observation of a hysteresis also in the low-pressure experiment suggests that the desorption of nitrogen from polymeric pore walls needs generally more investigation, and further experiments are necessary to clarify this phenomenon.

The BJH analysis of the adsorption branch of the isotherms revealed that all samples display monomodal pore sizes varying between 8 and 23 nm (see Figure 1c and Figure S7). The smallest pore sizes (8.4 nm) were found for the highly cross-linked samples, whereas samples with a low degree of cross-linking displayed larger pore sizes (up to 23 nm).

Figure 2 shows the SAXS patterns of the pressed pellet and the three selected materials (PS80DVB, PS10DVB, and PS0DVB). All the investigated materials displayed a pronounced Porod decay which allowed the extraction of the

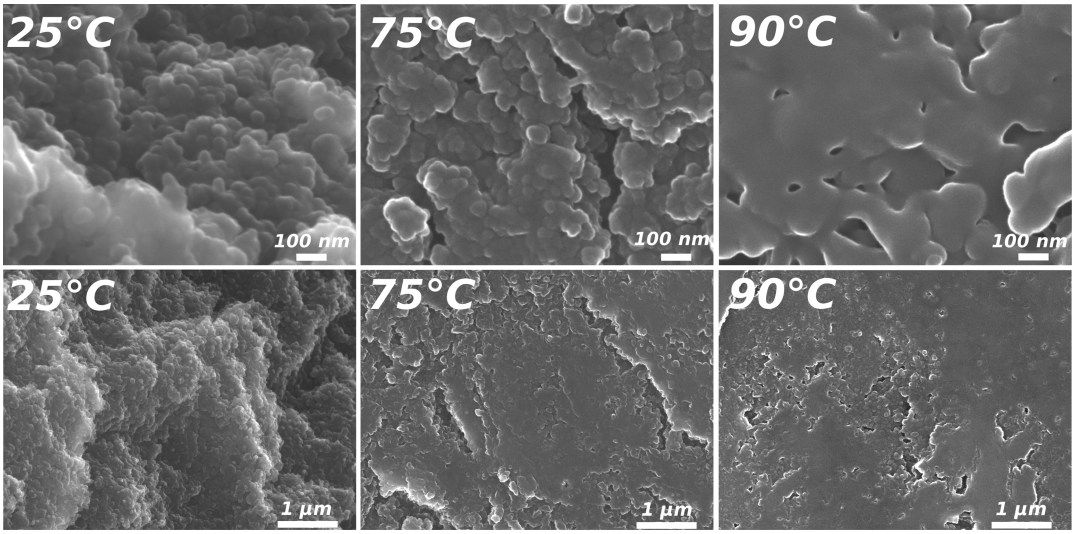

Figure 4. SEM micrographs of mesoporous non-cross-linked PS samples with varying thermal history (first column: 25 °C; second column: 75 °C; third column: 90 °C; first row: magnification ×100 000; scale bar: 100 nm; second row: magnification ×20 000; scale bar: 1 μm).

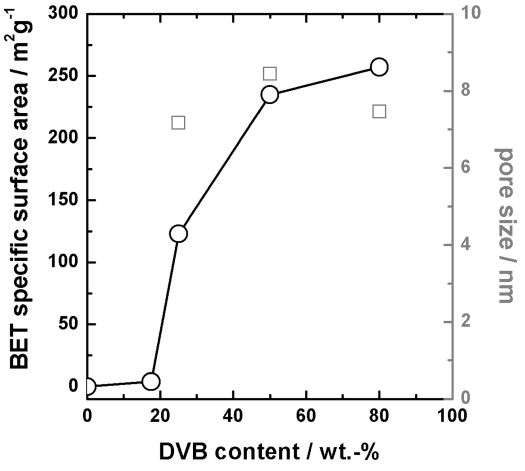

Figure 5. Specific surface areas (circles) as determined by the BET model and BJH model derived pore sizes (squares) of THF extracted samples as a function of the DVB content.

specific surface area S_{SAXS} and the pore and wall size as summarized in Table 1 and Figure 1b,c. Generally, the values obtained by evaluation of the SAXS data were in good to very good agreement with those calculated from the nitrogen sorption data. This indicates the absence of closed porosity; i.e., all pores are accessible to gas (and guest) molecules.

Furthermore, a replication of the initial morphology by structural inversion can be confirmed as the average wall thickness ($\langle l_{wall} \rangle \sim 20$ nm) of the polymeric samples corresponds fairly to the pore size of the pressed pellet ($\langle l_{pore} \rangle \sim 24$ nm). This holds especially true for materials of higher cross-linking density, while the inversion gets blurred at lower cross-linking due to the increasing pore size.

It is also interesting to note that there are additional features in the SAXS patterns of the PS10DVB and PS0DVB samples that are indicative for polydisperse spherical objects. Although a transformation into a spherical morphology may be driven by minimization of the interface energy, this conjecture suggests that such a morphological change happens well below the nominal glass transition temperature (T_g) of PS. Previous work has shown that the glass transition temperature is reduced as the polymer dimension is reduced to very small dimensions, i.e., to some tens of nanometers.[30−32]

Preliminary differential scanning calorimetric (DSC) measurements on non-cross-linked poly(styrene) showed no signal for temperatures below 65−70 °C, suggesting that the T_g is at least higher than 65 °C (see Figure S9). This is in accordance with previous estimates of the reduction of T_g found in thin films of low-M_w PS.[32] Although a pore related T_g reduction cannot be proven by DSC, as the first heating run shows only an ill-defined peak and the pores are closed after the material is heated above T_g, it is still plausible and needs to be considered. It is also possible that the polymerization reaction in confined space may introduce a stress in the polymers that is relieved by the observed morphological change.

Mesoporous non-cross-linked PS was subjected to various temperature treatments and analyzed by nitrogen sorption after being degassed for ~20 h under vacuum at 25, 60, 75, or 90 °C. Figure 3 shows that the specific surface area as well as the porosity becomes progressively smaller as the degassing temperature is increased.

The material degassed at 90 °C shows a nearly complete pore collapse as indicated by the rather low surface area ($S_{BET} = 28$ m^2 g^{-1}). The highest surface area was found for the material degassed at 25 °C ($S_{BET} = 180.5$ m^2 g^{-1}). The surface area was reduced to $S_{BET} = 155.6$ m^2 g^{-1} when degassing at 60 °C and was even more reduced by degassing at 75 °C ($S_{BET} = 87.2$ m^2 g^{-1}). It should be noted that the average pore size as determined by BJH analysis was comparable for all samples (23−27 nm). Hence, this again suggests that the T_g of the mesoporous PS is lower than the bulk value ($T_{g,onset} \sim 95$ °C) as complete or significant partial pore collapse can be observed at temperatures ≥75 °C.

The SEM investigation of PS samples with varying thermal history shows that an increase in temperature above 25 °C results in an progressive loss of the irregular-shaped surface with feature sizes well below 50 nm (Figure 4). Samples heated up to 75 °C still display a well-defined surface texture, but the size of the featureless regions has grown and one can find areas that have fused together. PS that was heated up to 90 °C shows a nearly complete loss of the original morphology with large fused areas.

Finally, the impact of the time scale was examined. One material (PS0DVB) was subjected to 60 °C for an extended time, and the surface area was measured after 2 and 6 days. It was found that the surface area and porosity were not

Table 2. Characteristics of Porous PS Polymers of Varying Cross-Linking Degree after THF Extraction

sample	V_{pore}[a] [cm^3 g^{-1}]	ϕ	S_{BET} [m^2 g^{-1}]	S_{SAXS} [m^2 g^{-1}]	d_{pore}[b] [nm]	l_p [nm]	$\langle l_{pore}\rangle$ [nm]	$\langle l_{wall}\rangle$ [nm]
PS80DVB_THF	0.45	0.32	257		7.46			
PS50DVB_THF	0.49	0.34	235	201.26	8.45	6.42	9.72	18.93
PS25DVB_THF	0.23	0.19	123	107.34	7.3	6.9	8.57	35.49
PS17.5DVB_THF			4			6.85		

[a] Determined at $p/p_0 = 0.99$. [b] BJH average (analysis of the adsorption branch).

affected by the additional heating time. This indicates that the time scale of the morphological changes is rather short.

After the material had been kept at 60 °C for 6 days, the temperature was increased to 70 °C for 1 day, and it was investigated by nitrogen sorption again. This yielded in a significant decrease of the surface area and porosity, which suggests that the average T_g of this porous polymer is around 70 °C. Because the pore and pore wall sizes are polydisperse, it is expected that the material should display a local variation in T_g. Small pore walls should thus collapse at lower temperatures. As a consequence, one can observe a slow breakdown of the porosity as the temperature gets nearer and nearer to the bulk T_g.

Mesopore Stability against Solvent Treatment. Usually, the purification of polymer networks involves the removal of synthesis residues by solvent treatment. Therefore, it is of interest to determine which cross-linking density is needed to ensure stability against solvent-induced pore collapse. Porous PS polymers of varying cross-linking density were extracted with THF. The solvent was afterward allowed to evaporate slowly at room temperature. The surface area retrieved from nitrogen sorption analysis showed that the stability threshold was around 20−25 wt % DVB (see Figure 5); below this cross-linking level the surface area is significantly reduced. It is interesting to note that the specific surface areas of highly cross-linked samples (≥50 wt % DVB) actually increased by the THF treatment.[33] Most likely, this is due to some microporosity, i.e., pores smaller than 2 nm, which became accessible after solvent extraction of the "nascent" polymers. Indeed, the pore volume of these samples showed only a very small increase compared to the nascent state. If the amount of DVB was reduced to 25 wt %, the surface area and porosity dropped after the THF extraction by almost a factor of 2, indicating partial pore collapse. The pore size of the remaining pores was however comparable to that of samples of higher DVB content. This finding indicates that pore collapse is a critical process; i.e., pores are either completely closed or remain virtually unaffected.[14]

Finally, the PS polymer containing 17.5 wt % DVB did not possess any porosity that could be probed by nitrogen sorption. However, this sample showed a SAXS pattern and a Porod length l_p comparable to the samples of higher cross-linking density, which suggests that the material contains closed pores (see Figure S11). This finding is in accordance with recent reports on "traced" porosity, i.e., a state between full collapse and permanent porosity.[21] It was shown that such samples, although they appeared to be mostly nonporous, could swell in a thermodynamically poor solvent. A possible explanation for this behavior might be related to the stress introduced into the polymer network by elastic pore closure. Swelling (of the closed pores), even with a poor solvent, would allow a minimization of this stress. Further studies, potentially employing cryoporometry might help to enlighten the phenomena. Table 2 summarizes the data of THF-treated samples.

As the nominal cross-linking density at which pore collapse started was found to be rather high, an explanation of the overall findings might consider an inhomogeneous cross-linking density, a fact which is generally accepted for polymer networks synthesized by free-radical polymerization,[34,35] as well as the nanosized dimensions of the pore walls. It can be expected that regions of low cross-linking density exist and that these are most prone to pore collapse as they are most flexible. It is, however, difficult to transfer the classic picture to the present system, as the polymerization and the associated phase separation processes are expected to be different in the confined space of the silica mesopores. Indeed, analysis of the bulk and mesoporous non-cross-linked PS by gel permeation chromatography (GPC) revealed that both samples had comparable molecular weights ($M_w \sim 150\,000$ g mol^{-1}), but different polydispersities and weak microgel formation are suspected for the PS synthesized in confinement.

Additionally, the pore walls are polydisperse in size, and it can be expected that smaller pore walls are less stable than larger ones. Hence, the action of both effects will determine the onset of pore collapse. A more detailed discussion and investigation of this issue would however be out of the scope of this article and will therefore not be covered at this stage.

Conclusions and Outlook

Mesoporous poly(styrene) and poly(styrene-*co*-divinylbenzene) networks could be synthesized using a new hard-templating approach. Commercially available fumed silica was pressed into a pellet, whose mesopores could then be infiltrated with the monomer/initiator mixture. The mesoporous polymers displayed specific surfaces areas up to 215 m^2 g^{-1} and porosities up to ∼35 vol % after polymerization and etching of the silica with aqueous NaOH.

At very high cross-linking density, one finds a near-perfect replication of the template, resulting in polymers with pore sizes around 10 nm. As the cross-linking degree is lowered, the pore size increases and the specific surface area is consequently decreased. For materials of very low DVB content, the pore sizes increase is very prominent, and pore sizes are increased up to ∼25 nm.

Studies of the temperature dependence on the pore stability of non-cross-linked PS indicate that at least two different processes are involved in the observed morphological changes and structural collapse.

The time scale for the observed morphological changes in the glassy state is rather short, which may be related to the release of internal stress. The coarsening of the characteristic features becomes more pronounced the lower the cross-linking density (the higher the flexibility) is. Comparison with previous results suggests that the low-temperature structural changes may be typical for the hard-templating route, i.e., the polymerization within confinement. Mesoporous polymers derived by "soft" block copolymer templating are usually prepared from equilibrated, microphase-separated block copolymers.[5] Hence, the internal stress is already minimized, and less dramatic changes are thus expected.

Second, it was found that subjecting the nascent mesoporous PS to temperatures well below the nominal T_g of the bulk material resulted in partial pore collapse. This can be explained by a lowering of T_g due to the nanosized dimensions. The effect of the polydispersity of the pore and pore wall sizes on the pore closure needs, however, further investigations.

Treatment of the mesoporous networks with THF resulted in pore collapse if the DVB content was lower than ~20 wt %. The pore collapse was found to be critical; i.e., no homogeneous shrinking of pores was found. Pores either collapse completely or keep their original size. However, there was evidence of the so-called traced porosity, i.e., pores that might be not accessible or can be reopened by solvent contact. These findings are pretty well in accordance with previous studies.[14,21]

Elucidating the determining factors that control pore stability is important for many potential applications of porous polymers, e.g., chromatography. Ongoing work on the issue of traced porosity is devoted to investigate swollen gels by cryoporometry.[36,37]

Finally, we would like to state the used hard-templating procedure can easily be extended toward other polymer classes. For instance, it is possible to prepare a mesoporous poly(ethylene glycol dimethacrylate) (PEGDMA) network. The network showed almost the same porosity ($S_{BET} = 200\ m^2\ g^{-1}$; BJH pore size: 9.7 nm) as the fully cross-linked DVB network (see Figure S12). Currently, we are studying the synthesis and properties of various mesoporous poly(acrylates) using the here presented hard-templating of fumed silica.

Acknowledgment. We thank Daniel Grüner and Kjell Jansson (SU) for assistance with SEM measurements. Yao Cheng (SU) is acknowledged for the TEM investigation of the fumed silica powder. Anwar Ahniyaz (YKI Stockholm, Sweden) is acknowledged for providing access to DSC. We thank Helmut Schlaad and Marlies Gräwert (MPI of Colloids and Interfaces, Potsdam, Germany) for performing the GPC measurements. The Wallenberg foundation is acknowledged for generous support of the electron microscopy and AFM facilities and the Stockholm University research center on porous materials, EXSELENT, for partial financial support. Jens Weber acknowledges financial support from the German Research Foundation (DFG, Grant WE-4504/1-1).

Supporting Information Available: Further analytical data including AFM, SEM, and TEM micrographs, DSC traces, GPC measurements, nitrogen sorption isotherms, and SAXS patterns. This material is available free of charge via the Internet at http://pubs.acs.org.

References and Notes

(1) Schuth, F. *Chem. Mater.* **2001**, *13*, 3184–3195.
(2) Davis, M. E. *Nature* **2002**, *417*, 813–821.
(3) Soler-illia, G. J. D.; Sanchez, C.; Lebeau, B.; Patarin, J. *Chem. Rev.* **2002**, *102*, 4093–4138.
(4) Schuth, F. *Angew. Chem., Int. Ed.* **2003**, *42*, 3604–3622.
(5) Olson, D. A.; Chen, L.; Hillmyer, M. A. *Chem. Mater.* **2008**, *20*, 869–890.
(6) Thomas, A.; Goettmann, F.; Antonietti, M. *Chem. Mater.* **2008**, *20*, 738–755.
(7) Thomas, A.; Kuhn, P.; Weber, J.; Titirici, M. M.; Antonietti, M. *Macromol. Rapid Commun.* **2009**, *30*, 221–236.
(8) Lee, J. S.; Hirao, A.; Nakahama, S. *Macromolecules* **1988**, *21*, 274–276.
(9) Hentze, H. P.; Antonietti, M. *Curr. Opin. Solid State Mater. Sci.* **2001**, *5*, 343–353.
(10) Hasegawa, J.; Kanamori, K.; Nakanishi, K.; Hanada, T.; Yamago, S. *Macromolecules* **2009**, *42*, 1270–1277.
(11) Goltner, C. G.; Weissenberger, M. C. *Acta Polym.* **1998**, *49*, 704–709.
(12) Johnson, S. A.; Ollivier, P. J.; Mallouk, T. E. *Science* **1999**, *283*, 963–965.
(13) Kim, J. Y.; Yoon, S. B.; Kooli, F.; Yu, J. S. *J. Mater. Chem.* **2001**, *11*, 2912–2914.
(14) Weber, J.; Antonietti, M.; Thomas, A. *Macromolecules* **2007**, *40*, 1299–1304.
(15) Deryo-Marczewska, A.; Goworek, J.; Zgrajka, W. *Langmuir* **2001**, *17*, 6518–6523.
(16) Pevida, C.; Drage, T. C.; Snape, C. E. *Carbon* **2008**, *46*, 1464–1474.
(17) Zalusky, A. S.; Olayo-Valles, R.; Taylor, C. J.; Hillmyer, M. A. *J. Am. Chem. Soc.* **2001**, *123*, 1519–1520.
(18) Garcia-Diego, C.; Cuellar, J. *Ind. Eng. Chem. Res.* **2005**, *44*, 8237–8247.
(19) Cavicchi, K. A.; Zalusky, A. S.; Hillmyer, M. A.; Lodge, T. P. *Macromol. Rapid Commun.* **2004**, *25*, 704–709.
(20) Muralidharan, V.; Hui, C. Y. *Macromol. Rapid Commun.* **2004**, *25*, 1487–1490.
(21) Guo, F.; Andreasen, J. W.; Vilgild, M. E.; Ndoni, S. *Macromolecules* **2007**, *40*, 3669–3675.
(22) Perret, R.; Ruland, W. *Kolloid Z. Z. Polym.* **1971**, *247*, 835–843.
(23) Sing, K. S. W.; Everett, D. H.; Haul, R. A. W.; Moscou, L.; Pierotti, R. A.; Rouquerol, J.; Siemieniewska, T. *Pure Appl. Chem.* **1985**, *57* (4), 603–619.
(24) Rouquerel, F.; Rouquerel, J.; Sing, K. S. W. Adsorption from Gas Phase. In *Handbook of Porous Solids*; Schüth, F., Sing, K. S. W., Weitkamp, J., Eds.; Wiley-VCH Verlag GmbH: Weinheim, 2002.
(25) Smarsly, B.; Groenewolt, M.; Antonietti, M. *Prog. Colloid Polym. Sci.* **2005**, *130*, 105–113.
(26) POWDER TECH NOTE 36, Quantachrome Instruments.
(27) Thommes, M.; Smarsly, B.; Groenewolt, M.; Ravikovitch, P. I.; Neimark, A. V. *Langmuir* **2006**, *22*, 756–764.
(28) Deryło-Marczewska, A.; Goworek, J.; Pikus, S.; Kobylas, E.; Zgrajka, W. *Langmuir* **2002**, *18*, 7538–7543.
(29) Tsujita, Y. *Prog. Polym. Sci.* **2003**, *28*, 1377–1401.
(30) de Gennes, P. G. *Eur. Phys. J. E* **2000**, *2*, 201–205.
(31) Dalnoki-Veress, K.; Forrest, J. A.; Murray, C.; Gigault, C.; Dutcher, J. R. *Phys. Rev. E* **2001**, *63*, 031801.
(32) Forrest, J. A.; Dalnoki-Veress, K. *Adv. Colloid Interface Sci.* **2001**, *94*, 167–196.
(33) The surface areas determined by the BET equation should be read as BET equivalent surface areas, as the BET model is not fully applicable if ultramicropores are present in the system.
(34) Bastide, J.; Leibler, L. *Macromolecules* **1988**, *21*, 2647–2649.
(35) Shibayama, M. *Bull. Chem. Soc. Jpn.* **2006**, *79*, 1799–1819.
(36) Wang, J.; Gonzalez, A. D.; Ugaz, V. M. *Adv. Mater.* **2008**, *20*, 4482–4489.
(37) Petrov, O. V.; Furó, I. *Prog. Nucl. Magn. Reson. Spectrosc.* **2009**, *54*, 97–122.